JLB

Article

Determining the role of mononuclear phagocytes in prion neuroinvasion from the skin

Gwennaelle J. Wathne, Adrien Kissenpfennig,† Bernard Malissen,‡ Chiara Zurzolo,§ and Neil A. Mabbott*,1*

*The Roslin Institute and Royal (Dick) School of Veterinary Sciences, University of Edinburgh, United Kingdom; †Centre for Infection and Immunity, School of Medicine, Dentistry and Biomedical Sciences, Queen's University of Belfast, Northern Ireland, United Kingdom; ‡Centre d'Immunologie de Marseille-Luminy, Université de la Méditerranée, INSERM, U631, CNRS, UMR6102 Case 906, Cedex, France; and §Institut Pasteur, Unité Trafic membranaire et Pathogenèse, Paris Cedex, France

RECEIVED DECEMBER 20, 2011; REVISED FEBRUARY 8, 2012; ACCEPTED FEBRUARY 9, 2012. DOI: 10.1189/jlb.1211633

ABSTRACT

Many prion diseases are acquired by peripheral exposure, and skin lesions are an effective route of transmission. Following exposure, early prion replication, upon FDCs in the draining LN is obligatory for the spread of disease to the brain. However, the mechanism by which prions are conveyed to the draining LN is uncertain. Here, transgenic mice were used, in which langerin$^+$ cells, including epidermal LCs and langerin$^+$ classical DCs, were specifically depleted. These were used in parallel with transgenic mice, in which nonepidermal CD11c$^+$ cells were specifically depleted. Our data show that prion pathogenesis, following exposure via skin scarification, occurred independently of LC and other langerin$^+$ cells. However, the depletion of nonepidermal CD11c$^+$ cells impaired the early accumulation of prions in the draining LN, implying a role for these cells in the propagation of prions from the skin. Therefore, together, these data suggest that the propagation of prions from the skin to the draining LN occurs via dermal classical DCs, independently of langerin$^+$ cells. *J. Leukoc. Biol.* 91: 817–828; 2012.

Introduction

Prion diseases (transmissible spongiform encephalopathies) are subacute neurodegenerative diseases that affect humans and animals. Many prion diseases, including natural sheep scrapie, bovine spongiform encephalopathy, chronic wasting disease in cervids, and variant Creutzfeldt-Jakob disease in humans, are acquired peripherally, for example, orally or by lesions to skin and mucous membranes. After peripheral exposure, prions first replicate upon FDC, as they make their journey from the site of infection to the CNS (a process, termed neuroinvasion) [1–6]. Prion replication upon FDC appears to be critical for efficient neuroinvasion [7–10]. During prion disease aggregations of PrP^{Sc}, an abnormally folded isoform of the PrP^{C}, accumulates in affected tissues. Prion infectivity copurifies with PrP^{Sc} and is considered to constitute the major, if not sole, component of an infectious agent [11, 12]. Host cells must express cellular PrP^{C} to sustain prion infection, and FDCs express high levels of PrP^{C} on their surfaces [10]. Although low levels of prion infectivity are present in the bloodstream of infected animals [13], prions appear to invade the CNS by spreading from lymphoid tissue via the peripheral nervous system [14].

Our data show that prion replication upon FDC within the draining LN is crucial for efficient neuroinvasion after exposure via skin scarification. For prions to replicate upon FDC, they must first be propagated from the site of exposure (skin) to the draining LN. The mechanism by which prions are delivered to the draining LN to establish infection upon FDC is uncertain. The identification of the cells and molecules involved in the propagation of prions may identify important processes that influence disease susceptibility and to which intervention strategies can be developed.

The skin is rich in mononuclear phagocytes, which continually survey the tissue for antigens and pathogens. Upon antigen encounter, these cells exit the skin via the afferent lymphatics and travel to the draining LN, where they present the antigen to T cells [15]. Within the epidermis are situated LCs,

Abbreviations: Alexa-PrP^{Sc}=fluorescently labeled relatively proteinase-resistant, disease-specific form of the prion protein, CR1=complement receptor 1, dH_2O=distilled H_2O, DTR=diphtheria toxin receptor, DTX=diphtheria toxin, FDC=follicular DC, GFAP=glial fibrillary acidic protein, Iba-1=ionized calcium-binding adaptor molecule 1, IHC=immunohistochemistry, PB=phosphate buffer, PET=paraffin-embedded tissue immunoblot, PrP^{C}=cellular isoform of prion protein, PrP^{d}=disease-specific isoform of prion protein detected by immunohistochemistry, PrP^{Sc}=relatively proteinase-resistant, disease-specific form of the prion protein, SCS=subcapsular sinus, ZO-1=zonula occludens-1

The online version of this paper, found at www.jleukbio.org, includes supplemental information.

1. Correspondence: The Roslin Institute and Royal (Dick) School of Veterinary Sciences, University of Edinburgh, Easter Bush, Midlothian EH25 9RG, UK. E-mail: neil.mabbott@roslin.ed.ac.uk

which express high levels of langerin (CD207) and were long considered to be the exclusive APCs of the skin. However, the skin has been shown to contain other important subsets of mononuclear phagocytes, termed dermal DCs. Based on their expression of langerin, CD11c, CD11b, and CD103, five distinct skin mononuclear phagocyte subsets have since been described [16]. The capacity of LCs and dermal DCs to migrate to the draining LN under steady-state and inflammatory conditions, the demonstration that LC can acquire dengue virus after exposure via the skin [17], data suggesting lung $CD103^+$ DCs can transport influenza virus to the draining LN [18], and data showing that the depletion of $CD11c^+$ cells impaired prion neuroinvasion from the intestine [19] and peritoneal cavity [20] suggested that skin mononuclear phagocytes were ideal candidates to propagate prions from the skin.

In the current study, langerin-DTR transgenic mice [21] and CD11c-DTR-transgenice mice [22] were used. In each of these transgenic mouse models, treatment with DTX transiently depletes the DTR-expressing cells in vivo: $CD11c^+$ cells in CD11c-DTR mice; $langerin^+$ cells in langerin-DTR mice. FDCs are unaffected by DTX treatment in these transgenic mouse models, as they do not express CD11c or langerin. These transgenic mouse models were used in parallel to determine the potential role of distinct mononuclear phagocyte populations in the propagation of prions to the draining LN after exposure via skin lesions.

MATERIALS AND METHODS

Mice

CD11c-DTR [22] and langerin-DTR [21] (6–8 weeks old) were bred and maintained on a C57BL/6 background under specific pathogen-free conditions. Where indicated, bone marrow from the femurs and tibias of donor mice was prepared as a single-cell suspension (3×10^7–4×10^7 viable cells/ml) in HBSS (Invitrogen, Paisley, UK). Recipient adult (6–8 weeks old) mice were γ-irradiated (1000 rad) and 24 h later, reconstituted with 0.1 ml bone marrow by injection into the tail vein. Recipient mice were used in subsequent experiments 8 weeks after bone marrow grafting. All studies using experimental mice and regulatory licenses were approved by The Roslin Institute's and University of Edinburgh's Protocols and Ethics Committees. All animal experiments were carried out under the authority of a UK Home Office Project License within the terms and conditions of the strict regulations of the UK Home Office Animals (scientific procedures) Act 1986.

Treatment with DTX

DTX was suspended in 5% lactose in 10 mM PB. CD11c-DTR mice were given a single i.p. injection of 100 ng/mouse DTX (Sigma-Aldrich, Dorset, UK) to deplete their $CD11c^+$ cells. Langerin-DTR mice were injected i.p. with 1 μg/mouse DTX to deplete their $langerin^+$ cells. Some mice were injected with PB as a control.

Prion exposure and disease monitoring

Mice were inoculated with ME7 scrapie prions by skin scarification of the medial surface of the left thigh [3, 4, 23]. Briefly, prior to scarification, ~1 cm^2 area of hair covering the site of scarification was trimmed using curved scissors and then removed completely with an electric razor. Twenty-four hours later, a 23-gauge needle was used to create a 5-mm-long abrasion in the epidermal layers of the skin at the scarification site. Then, using a 26-gauge needle, one droplet (~6 μl) of prion inoculum from a 1.0% (wt/vol) terminal scrapie mouse brain homogenate in physiological saline was applied to the abrasion and worked into the site using sweeping strokes. The scarification site was then sealed with OpSite (Smith & Nephew Medical, Hull, UK) and allowed to dry before the animals were returned to their final holding cages. Following inoculation, all animals were coded, assessed weekly for signs of clinical disease, and killed at a standard clinical end-point [24]. Scrapie diagnosis was confirmed by histopathological assessment of spongiform pathology in the brain. For the construction of lesion profiles, vacuolar changes were scored in nine gray-matter areas of brain as described [25]. Where indicated, some mice were culled at the times indicated postinjection, with prions and tissues taken for further analysis.

Preparation of Alexa-PrP^{Sc}

Alexa fluor 546-conjugated PrP^{Sc} was prepared as described [26] with modification. Isolation of scrapie-associated PrP^{Sc} fibrils: brain homogenates 10% (wt/vol) in 0.01 M sodium phosphate, pH 7.4, plus 10% sarcosine were prepared from mice terminally affected with ME7 scrapie prion disease and centrifuged for 2.5 h at 215,000 *g*. Supernatants were discarded and pellets suspended in 3 ml dH_2O and incubated at room temperature for 1 h. Iodide solution (6 ml; 0.9 M potassium iodide, 9 mM sodium thiosulphate, 15 mM sodium phosphate, pH 8.5, with HCl, 1% sarcosine) was added to the samples. They were then layered onto a 3-ml sucrose cushion (20% sucrose in iodide solution) and centrifuged at 10°C for 90 min at 285,000 *g*. Supernatants were discarded, and pellets were suspended in 1 ml 0.1% Sarkosyl/PBS and centrifuged at room temperature for 30 min at 13,000 *g*. Pellets were resuspended in 20 μl 0.1% Sarkosyl/PBS and sonicated (Ultrasonic Processor XL, Qsonica, Newtown, CT, USA) in 10-s bursts to aid suspension.

Fluorescent labeling

Next, Alexa-fluor 546 succinimidyl ester (Invitrogen) was added (1 vol Alexa-fluor 546:10 vol sample) and incubated at room temperature for 1 h with constant agitation (in the dark). The reaction was quenched overnight at 4°C by adding 1 vol 1.5 M hydroxylamine (pH 8.5) to 10 vol dye reaction. Labeled samples were washed extensively in 0.1% Sarkosyl/PBS at room temperature for 10 min at 13,000 *g* to ensure that the supernatant of the final wash was clear and colorless. Pellets were resuspended in 20 μl 0.1% Sarkosyl/PBS, sonicated to aid suspension, and stored at −20°C until further use.

PK treatment

Samples were thawed and sonicated in 10-s bursts to aid suspension and PK added at a final concentration of 100 ng/ml. Samples were incubated at 37°C for 1 h with constant agitation, and the reaction stopped with 2 mM PMSF (Sigma-Aldrich). Samples were then diluted to 1 ml with 0.1% Sarkosyl/PBS, washed, and stored at −20°C until use.

Analysis

Alexa-PrP^{Sc} samples, treated in the absence or presence of PK, were resuspended and electrophoresed through duplicate SDS/PAGE 12% gels (Invitrogen). Following electrophoresis, one gel was fixed in "fluorofix" (40% ethanol, 2% acetic acid in dH_2O), prior to imaging on a Typhoon fluorescent imager (GE Healthcare, Waukesha, WI, USA). Afterwards, the gel was fixed, washed, and silver-stained to reveal proteins. The second gel was transferred to a PVDF membrane (Bio-Rad Laboratories, Hemel Hempstead, UK) by semidry blotting. PrP was detected using the PrP-specific mAb 8H4 [27], followed by HRP-conjugated goat anti-mouse antibody. Bound HRP activity was detected by ECL.

IHC and immunofluorescent analyses

For wholemount analysis of the epidermis and dermis, ears were separated into dorsal and ventral halves. s.c. fat and cartilage were removed. Skin was floated on 3.8% ammonium thiocyanate in 100 mM sodium phosphate/100 mM potassium phosphate for 20 min at 37°C. Epidermal and dermal

sheets were then separated and fixed in acetone at −20°C for 15 min [28]. Prior to immunostaining, samples were permeabilized for 15 min in 0.1% saponin, 5% FCS in PBS, incubated with anti-langerin mAb (clone 929F3.01; Cambridge Bioscience, Cambridge, UK). For analysis of ZO-1 within tight junctions, ventral ear sheets were floated out, cartilage side down, in PBS containing 0.7 mM $Ca2^+$. s.c. fat and cartilage were removed, and tissues floated out in 95% ethanol on ice and incubated for 30 min. Ears were subsequently floated out, epidermis side up, onto 3.8% ammonium thiocyanate and incubated at 37°C for 17 min. Tissues were floated out in PBS, transferred onto glass slides (Superfrost slides, Thermo Scientific, UK), and immunostained with mouse anti-ZO-1 mAb (clone T8-754; [29].

LNs and spleens were removed and snap-frozen at the temperature of liquid nitrogen. Serial frozen sections (8 μm in thickness) were cut on a cryostat and immunostained with the following antibodies: FDC were visualized by staining with mAb 7G6 to detect CR2/CR1 (CD21/CD35; BD Biosciences, San Diego, CA, USA) and mAb 8C12 to detect CR1 (CD35; BD Biosciences). Cellular PrP^C was detected using PrP-specific pAb 1B3 [30]. B cells were detected using rat anti-mouse B220 mAb (clone RA3-RB2; Caltag, Towcester, UK). $CD11c^+$ cells were detected using hamster anti-mouse CD11c mAb (clone HL3; BD Biosciences). $CD169^+$ cells were detected using mAb MOMA-1 (AbD Serotec, Germany). Neutrophils were detected using Ly-6B-specific mAb (clone 7/4; AbD Serotec).

For the detection of PrP^d in LNs and brains, tissues were fixed in periodate-lysine-paraformaldehyde fixative and embedded in paraffin wax. Sections (thickness, 6 μm) were deparaffinised and pretreated to enhance the detection of PrP^d by hydrated autoclaving (15 min, 121°C, hydration) and subsequent immersion in formic acid (98%) for 5 min [31]. Sections were then immunostained with 1B3 PrP-specific pAb. For the detection of astrocytes, brain sections were immunostained with anti-GFAP (Dako, Ely, UK). For the detection of microglia, deparaffinised brain sections were first pretreated with Target Retrieval Solution (Dako) and subsequently immunostained with anti-Iba-1 (Wako Chemicals GmbH, Neuss, Germany). Immunolabeling was revealed using HRP conjugated to the avidin-biotin complex (Novared kit, Vector Laboratories, Peterborough, UK). PET immunoblot analysis was used to confirm that the PrP^d detected by IHC was PK-resistant PrP^{Sc} [32]. Membranes were subsequently immunostained with 1B3 PrP-specific pAb.

For light microscopy, following the addition of primary antibodies, biotin-conjugated, species-specific secondary antibodies (Stratech, Soham, UK) were applied, and immunolabeling was revealed using alkaline phosphatase conjugated to the avidin-biotin complex. Sections were counterstained with hematoxylin to distinguish cell nuclei. For fluorescent microscopy, following the addition of primary antibody, streptavidin-conjugated or species-specific secondary antibodies coupled to Alexa Fluor 488 (green), Alexa Fluor 594 (red), or Alexa Fluor 647 (blue) dyes (Invitrogen) were used. Sections were mounted in fluorescent mounting medium (Dako) and examined using a Zeiss LSM5 confocal microscope (Zeiss, Welwyn Garden City, UK).

For morphometric analysis, digital microscopy images were analyzed using ImageJ software (http://rsb.info.nih.gov/ij/). In each instance, tissues from three to four mice from each group were analyzed. From each mouse, the numbers of positively immunostained pixels in images from at least three randomly chosen fields of view were collected. Data are presented as mean ± SD, and significant differences between samples in different groups were sought by Student's *t* test. Values of $P < 0.05$ were accepted as significant.

Microarray analysis

Ear skin was collected into RNAlater (Ambion, Austin, TX, USA) and stored at −80°C prior to analysis. The quality of RNA for microarray analysis was first determined on an Agilent BioAnalyzer 2100 (Agilent Technologies, Santa Clara, CA, USA). RNA was reverse-transcribed to cDNA, amplified, and labeled using the Genechip 3′ IVT Express Labeling Kit (Affymetrix, Santa Clara, CA, USA), according to the manufacturer's instructions. Samples were hybridized to Mouse 430_2.0 Affymetrix chips (Affymetrix), stained, and scanned by ARK Genomics (Edinburgh, UK). Raw data (.cel) files were normalized using Robust Multichip Average (RMAExpress; http://rmaexpress.bmbolstad.com/). Probe sets were annotated using the latest libraries available from Affymetrix. Genes of interest were assessed for recognized homologies, cellular location, function, and gene ontology terms using publicly available, web-based analysis tools and databases, including: ENSEMBL (http://www.ensembl.org/index.html); Gene Set Enrichment Analysis Molecular Signatures Database (GSEA MSigDB; http://www.broadinstitute.org/gsea/ msigdb/index.jsp); GOstat (http://gostat.wehi.edu.au). The raw microarray data (.cel files) are deposited in the Gene Expression Omnibus (GEO) under the following accession number: GSE34955 (http://www.ncbi.nlm.nih.gov/geo/query/acc.cgi?acc=GSE34955).

Statistical analyses

Survival time data are presented as mean ± SE. Significant differences between groups were sought by ANOVA. Values of $P < 0.05$ were accepted as significant.

RESULTS

Specific depletion of nonepidermal $CD11c^+$ cells

To determine the contribution of mononuclear phagocyte populations in the propagation of prions from the skin to the draining LN, transgenic mouse models were used, in which these cells can be transiently depleted. First, we used CD11c-DTR mice to study the potential role of $CD11c^+$ cells [22]. In the mouse, CD11c is expressed by classical DC and at much lower levels by LC and $CD169^+$ macrophages. As a consequence, each of these populations is significantly depleted in CD11c-DTR mice after DTX treatment (**Fig. 1A**). Classical DCs, including those in the dermis, are considered to derive from hematopoietic precursors, whereas LCs, although of myeloid origin, appear to derive independently from the bone marrow [33]. Furthermore, in contrast to classical DCs, LCs, in the epidermis and certain other resident mononuclear phagocytes (e.g., $CD169^+$ macrophages), are long-lived and relatively radioresistant and remain in tissues following γ-irradiation. Therefore, as a result of their differing ontogeny and radioresistance, it is possible to mix and match the genotype of the LC and classical DC using bone marrow chimeric mice. Here, a mouse model was used in which nonepidermal $CD11c^+$ cells could be specifically depleted but not the LC in the epidermis. To do so, WT mice were lethally γ-irradiated and 24 h later, reconstituted with bone marrow from CD11c-DTR recipients (hereafter termed CD11c-DTR→WT mice). WT → WT mice were used as controls. Eight weeks after bone marrow reconstitution, mice were injected with DTX or PB as a control. In the skin of CD11c-DTR → WT mice, the LCs derive from the WT bone marrow and are refractory to DTX treatment (Fig. 1B; P=0.52), whereas the classical DCs in the dermis are derived from the CD11c-DTR host and are significantly depleted by DTX (Fig. 1B; P<0.004). Further analysis showed that whereas the $CD11c^+$ cells in the spleens of DTX-treated CD11c-DTR → WT mice were significantly depleted, the $CD169^+$ macrophages were not significantly affected (Fig. 1C; P<0.0005, and P=0.97 for $CD11c^+$ cells and $CD169^+$ macrophages, respectively).

Although these data show that the classical DCs were depleted almost entirely, some cells remained after DTX treat-

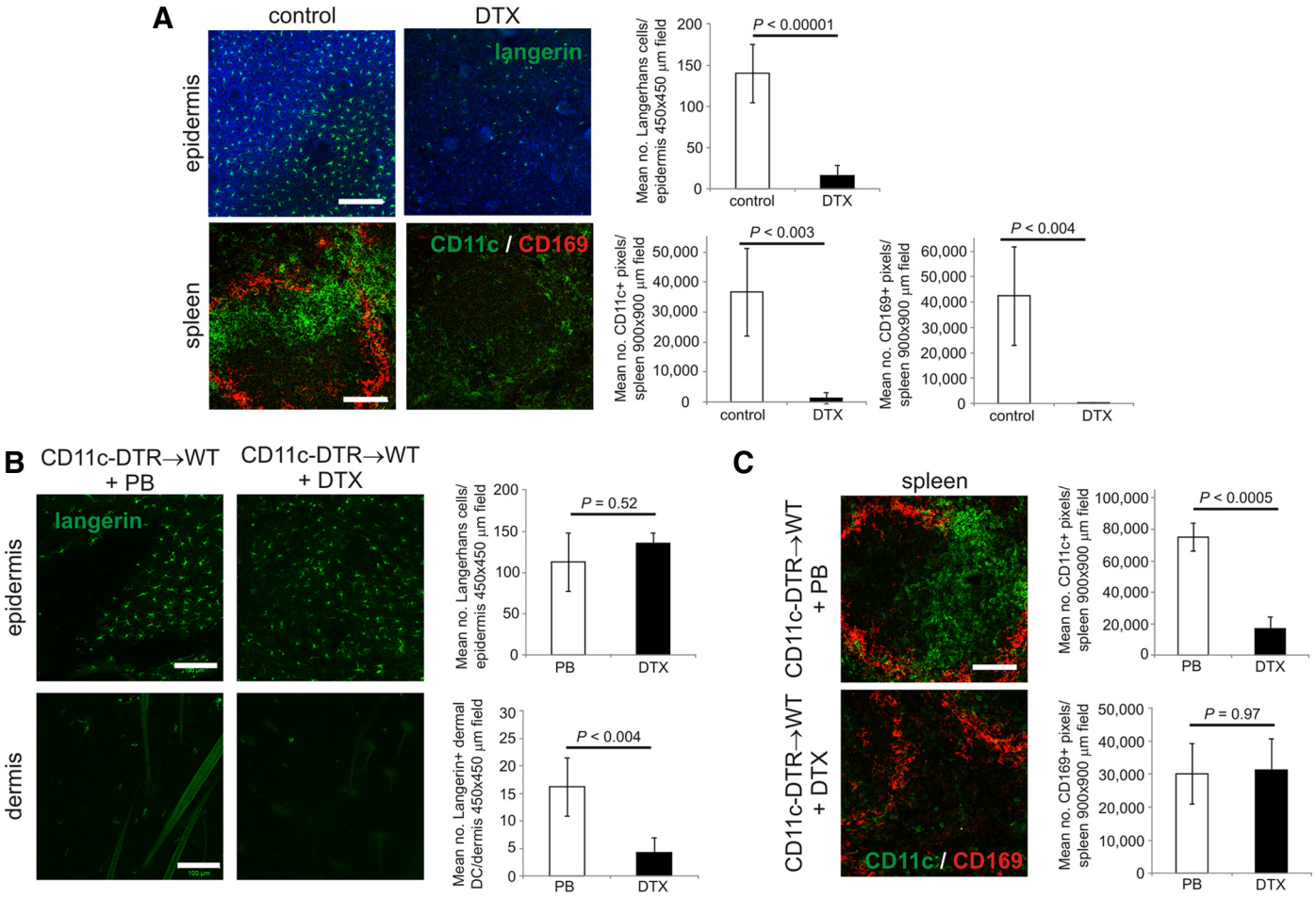

Figure 1. Effect of DTX treatment on the status of LCs, CD11c$^+$ cells, and CD169$^+$ cells in the tissues of CD11c-DTR → WT mice. (A) CD11c-DTR mice were treated with DTX or PB (control) and 2 days later, tissues analyzed by IHC. Epidermal LCs, classical CD11c$^+$ DCs, and CD169$^+$ macrophages are significantly depleted after DTX treatment of CD11c-DTR mice. (B and C) WT mice were lethally γ-irradiated and 24 h later, reconstituted with bone marrow from CD11c-DTR recipients (CD11c-DTR→WT mice). WT → WT mice were used as controls. Eight weeks after bone marrow reconstitution, mice were injected with DTX or PB as a control. Two days after treatment, tissues were analyzed by IHC. (B) LCs are unaffected by DTX treatment in the epidermis of CD11c-DTR → WT mice (B, upper panels). In contrast, nonepidermal langerin$^+$ classical DC in the dermis (B, lower panels) and CD11c$^+$ cells in the spleen (C) were significantly depleted by DTX treatment in CD11c-DTR → WT mice. Histograms show the effects of DTX treatment on mean the number of LCs in the epidermis and langerin$^+$ DCs in the dermis (expressed as mean no. cells ± SD/450×450 μm field of view) and the morphometric analysis of the mean number of CD11c$^+$ and CD169$^+$ pixels in images from spleens (expressed as mean no. positive pixels±SD/900×900 μm field of view). In each instance, three to four mice/group were analyzed and data collected from three to six images/mouse. Original scale bars = 100 μm.

ment. Previous data showed that in the LNs and spleen, the depletion of CD11c$^+$ cells is 60–80% efficient in CD11c-DTR mice [19, 22]. Why cell depletion in these tissues is not 100% effective is not known and may be influenced by a number of factors: differing expression levels of DTR on the target cells, differing cell-cycling kinetics in classical DC subpopulations, or simply, a result of the penetrance of the DTX. Despite extensive attempts, we were unable to readily detect CD11c$^+$ cells in the epidermis and dermis by whole-mount immunofluorescence. This was most likely a result of the very low expression level of CD11c by the cells with these tissues and the effects of the fixation and treatments used to prepare the epidermal and dermal sheets on the epitope recognized by the anti-CD11c mAb.

As prion replication upon PrP^C-expressing FDCs within the draining LN is important for efficient prion neuroinvasion after exposure via the skin [3, 4], we next determined the effect of DTX treatment on the status of FDC in CD11c-DTR → WT mice. FDCs in mice characteristically express high levels of CR1 (CD35) [34] and cellular PrP^C [10, 35, 36]. The expression of each of these molecules by FDC is important for the retention and replication of prions upon their surfaces. IHC analysis suggested that DTX treatment had no observable effect on the expression of PrP^C and CD35 by FDC within B cell follicles in the spleens (**Fig. 2**) and LNs (data not shown) of mice from each group. These data are consistent with the lack of expression of *Itgax* (which encodes CD11c) by FDC [37]. Together, these data confirm that classical DCs are

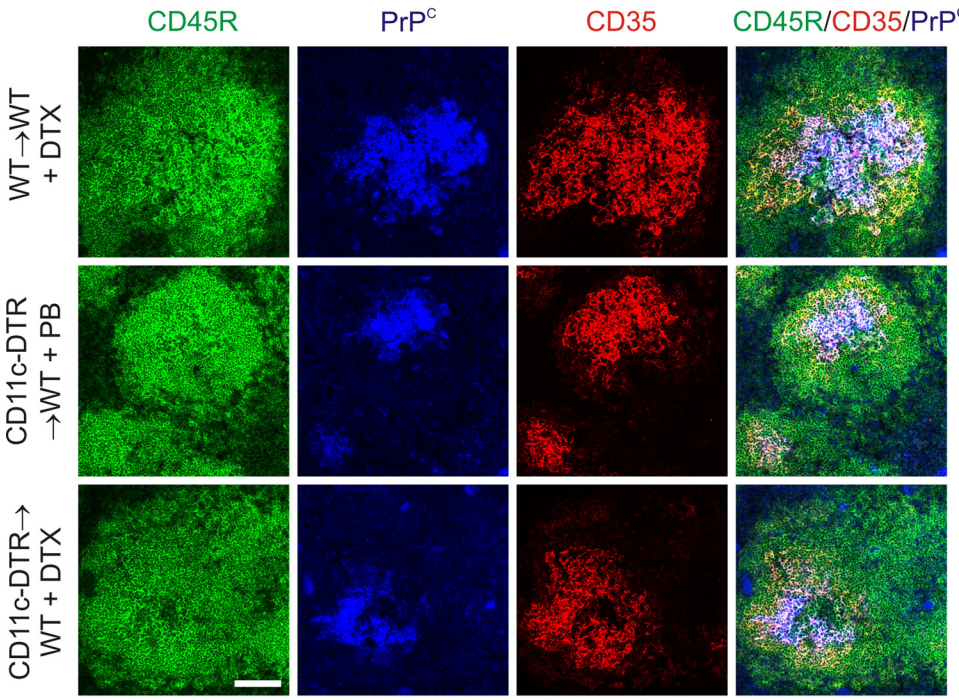

Figure 2. Treatment of CD11c-DTR → WT mice with DTX does not affect the status of FDC. IHC analysis of the expression of CD35 (red) and PrP^C (blue) suggested no observable effect of DTX treatment on the status of FDC in the B cell follicles (CD45R-expressing cells; green) in spleens from CD11c-DTR → WT mice. Data are representative of tissues from at least three mice/group. Original scale bar = 100 μm.

specifically and significantly depleted in DTX-treated CD11c-DTR → WT mice without affecting the status of LCs in the epidermis or $CD169^+$ macrophages and FDCs in lymphoid tissues.

Nonepidermal $CD11c^+$ cell depletion impairs the early accumulation of PrP^{Sc} upon FDC in the draining LN

Within weeks of exposure via skin scarification, ME7 scrapie prions accumulate, first upon FDC within the draining LNs and persist there at high levels until the terminal stages of disease [3, 4]. Therefore, we next determined the effect of classical DC depletion on the transfer of prions from the skin to the draining LN. Eight weeks after bone marrow reconstitution, CD11c-DTR → WT mice were injected with DTX to deplete their $CD11c^+$ cells and 2 days later, were exposed to ME7 scrapie prions by skin scarification. DTX-treated WT → WT mice and PB-treated CD11c-DTR → WT mice were used as controls.

In this study, the normal cellular form of PrP is referred to as PrP^C, and two distinct terms (PrP^{Sc} and PrP^d) are used to describe the disease-specific, abnormal accumulations of PrP, which are characteristically found only in prion-affected tissues. Prion disease-specific PrP accumulations are relatively resistant to PK digestion, whereas cellular PrP^C is destroyed. As a consequence, PK-resistant PrP (referred to as PrP^{Sc}) can be used as a biochemical marker for the presence of prions [11]. Unfortunately, the treatment of histological sections with PK destroys the tissue microarchitecture. Therefore, on histological sections, where PK was not applied, we refer to these disease-specific PrP accumulations as PrP^d. However, to confirm the presence of PrP^{Sc}, adjacent sections were applied to nitrocellulose membrane treated with PK and subsequently analyzed by PET immunoblot [32]. We have repeatedly shown in a series of studies that these PrP^d/PrP^{Sc} accumulations occur only in prion-infected tissues and correlate closely with the presence of ME7 scrapie prions [3, 7, 9, 10, 19, 35].

By 5 weeks after prion exposure, PrP^d accumulations, consistent with localization upon FDC within B cell follicles, were detected in the draining LNs from control mice (DTX-treated WT→WT mice and PB-treated CD11c-DTR→WT mice; n=3/group; **Fig. 3A** and **B**). PET immunoblot of adjacent histological sections confirmed the presence of high levels of PrP^{Sc} upon FDC in tissues from control mice (Fig. 3Ai and ii for tissues from DTX-treated WT→WT mice and PB-treated CD11c-DTR→WT mice, respectively). In contrast, in the absence of nonepidermal $CD11c^+$ cells at the time of prion exposure, PrP^{Sc} accumulation, within the draining LN, was impaired. No PrP^{Sc} was observed upon FDC in the draining LNs from two of three DTX-treated CD11c-DTR → WT mice (Fig. 3Aiv). Thus, in the absence of classical DC at the time of prion exposure, the early propagation of prions from the skin to the draining LN was impaired.

Effect of classical DC depletion on prion neuroinvasion

We next determined the effect of nonepidermal $CD11c^+$ cell depletion on prion disease susceptibility. All control mice (DTX-treated WT→WT mice and PB-treated CD11c-DTR→WT mice) succumbed to clinical prion disease with similar incubation periods, ~325 days after exposure (n=7/group; **Table 1**). In contrast, in the absence of classical DC at the time of exposure, survival time was delayed, as DTX-treated CD11c-DTR → WT mice succumbed to clinical prion disease, ~20 days later than control mice (Table 1), although

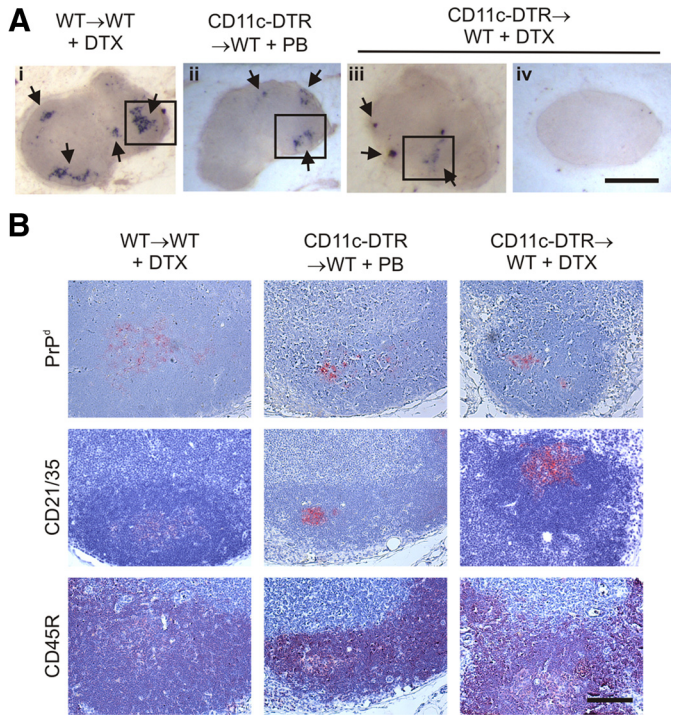

Figure 3. Prion accumulation in the draining LN is impaired in the absence of nonepidermal CD11$^+$ cells at the time of exposure. Eight weeks after bone marrow reconstitution, CD11c-DTR → WT mice were injected with DTX to deplete their CD11c$^+$ cells, and 2 days later, mice were exposed to ME7 scrapie prions by skin scarification. DTX-treated WT → WT mice and PB-treated CD11c-DTR → WT mice were used as controls. Draining LNs were collected 35 days postinfection (n=3 mice/group). (A) PET immunoblot analysis confirmed the presence of PK-resistant PrP^{Sc} (blue/black) upon FDC (arrows) in the draining LNs of control mice (DTX-treated WT→WT mice, i; PB-treated CD11c-DTR→WT mice, ii). In contrast, no PrP^{Sc} was detected in two of three of the LNs from the DTX-treated CD11c-DTR → WT mice, which lacked nonepidermal CD11c$^+$ cells at the time of exposure (iv), whereas some PrP^{Sc} was detected in the remaining LN from this treatment group (iii). (B) PrP^{Sc} detected in boxed areas in A is shown at greater magnification. IHC analysis confirmed that the PrP^d (red, top panels) was in association with FDC (CD21/35-expressing cells; red, middle panels) in the B cell follicles (CD45R-expressing cells; red, bottom panels) in LNs from control mice (DTX-treated WT→WT mice) and PB-treated CD11c-DTR → WT mice. Original scale bars = 500 μm (A); 100 μm (B).

the increase in survival time was not significantly different when compared with controls (P<0.099, Kruskall Wallis nonparametric ANOVA; n=7/group).

Characteristic spongiform pathology, astrogliosis, microgliosis, and PrP^{Sc} accumulation, typically associated with terminal infection with ME7 scrapie prions, were detected in the brains of each group of mice (**Fig. 4A**). Furthermore, the severity and distribution of the spongiform pathology within the brains of each group of mice were likewise typical of mice clinically affected with ME7 scrapie prions (Fig. 4B). Thus, CD11c$^+$ cell depletion at the time of prion exposure did not influence the magnitude or distribution of the neuropathology within the brains of clinically affected mice.

Specific depletion of langerin$^+$ cells

Next, we used langerin-DTR mice [21] to study the potential role of langerin$^+$ cells in prion neuroinvasion from the skin. In the skin, langerin (CD207) is expressed by the LC and dermal DC populations. Consistent with previous data [21], each of these populations is almost completely and significantly ablated in langerin-DTR mice within 2 days after DTX treatment (**Fig. 5A**; P<0.00001 for LC and langerin$^+$ dermal DC populations). However, whereas each cell population is depleted rapidly after DTX treatment, the langerin$^+$ dermal DCs repopulate the skin within 2 weeks after treatment. The LCs remain depleted for several weeks (Fig. 5B). As anticipated, IHC analysis suggested that there was no observable difference on the effects of DTX treatment of langerin-DTR mice on the expression of PrP^C and CD35 by FDCs in the LNs (Fig. 5C) and spleen (data not shown).

Effect of langerin$^+$ cell depletion on prion pathogenesis

Next, we determined the effect of langerin$^+$ cell depletion on the propagation of prions from the skin to the draining LN. Groups of langerin-DTR mice were injected with DTX to specifically deplete their langerin$^+$ cells. DTX-treated WT mice and PB-treated langerin-DTR mice were used as controls. Two days later, mice were exposed to ME7 scrapie prions by skin scarification. By 5 weeks after prion exposure, PrP^{Sc} accumulations, consistent with localization upon FDC, were detected in the draining LNs from each group of mice (**Fig. 6**). These data clearly show that langerin$^+$ cell depletion did not impair the early accumulation of prions within the draining LN.

We next determined the effect of langerin$^+$ cell depletion on prion disease susceptibility. Our data show that langerin$^+$ cell depletion had no significant effect on the spread of prions to the brain, as all mice succumbed to clinical prion disease with similar incubation periods (**Table 2**). Furthermore, the neuropathology within the brains of mice from each group was similar and typical of mice clinically affected with ME7 scrapie prions (**Fig. 7**). Together, these data clearly demonstrate that the specific depletion of langerin$^+$ cells does not influence prion neuroinvasion after exposure by skin scarification.

TABLE 1. Effect of Nonepidermal CD11c$^+$ Cell Depletion on Prion Disease Susceptibility

Group	Treatment[a]	Incidence[b]	Mean incubation period (days) ± SE
WT → WT	DTX	7/7	328 ± 7
CD11c-DTR → WT	PBS	7/7	324 ± 10
CD11c-DTR → WT	DTX	7/7	347 ± 5

[a] Mice were treated with DTX, 2 days before infection with ME7 scrapie prions via skin scarification. [b] Incidence, Number of animals affected with clinical prion disease/number of animals tested.

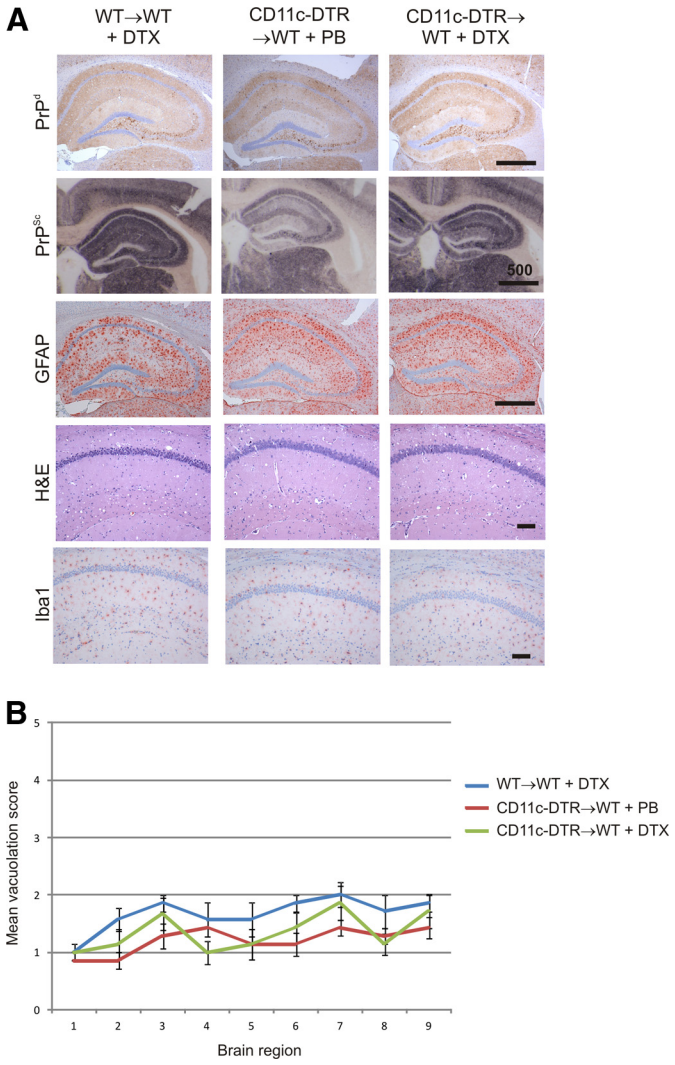

Figure 4. Effect of CD11$^+$ cell depletion on the development of neuropathology within the brain. Eight weeks after bone marrow reconstitution, CD11c-DTR → WT mice were injected with DTX to deplete their CD11c$^+$ cells, and 2 days later, mice were exposed to ME7 scrapie prions by skin scarification. DTX-treated WT → WT mice and PB-treated CD11c-DTR → WT mice were used as controls. Brains were collected from clinically, scrapie-affected mice at the end of the experiment and the neuropathology within each brain compared. (A) Heavy accumulations of disease-specific PrP (brown, top row), reactive astrocytes expressing GFAP (red, third row from top), high levels of spongiform pathology (H&E, fourth row from top), and active microglia-expressing Iba-1 (red, bottom row) were detected in the brains of all clinically, scrapie-affected mice. Analysis of adjacent sections by PET immunoblot analysis confirmed the presence of PK-resistant PrP^{Sc} (blue/black, second row from top). Original scale bars = 100 μm unless indicated. (B) Pathological assessment of the spongiform change (vacuolation) in brains from terminally scrapie-affected mice. Vacuolation was scored on a scale of 0–5 in the following gray matter areas: G1, dorsal medulla; G2, cerebellar cortex; G3, superior colliculus; G4, hypothalamus; G5, thalamus; G6, hippocampus; G7, septum; G8, retrosplenial and adjacent motor cortex; G9, cingulate and adjacent motor cortex. Data are representative of tissues from seven mice/group.

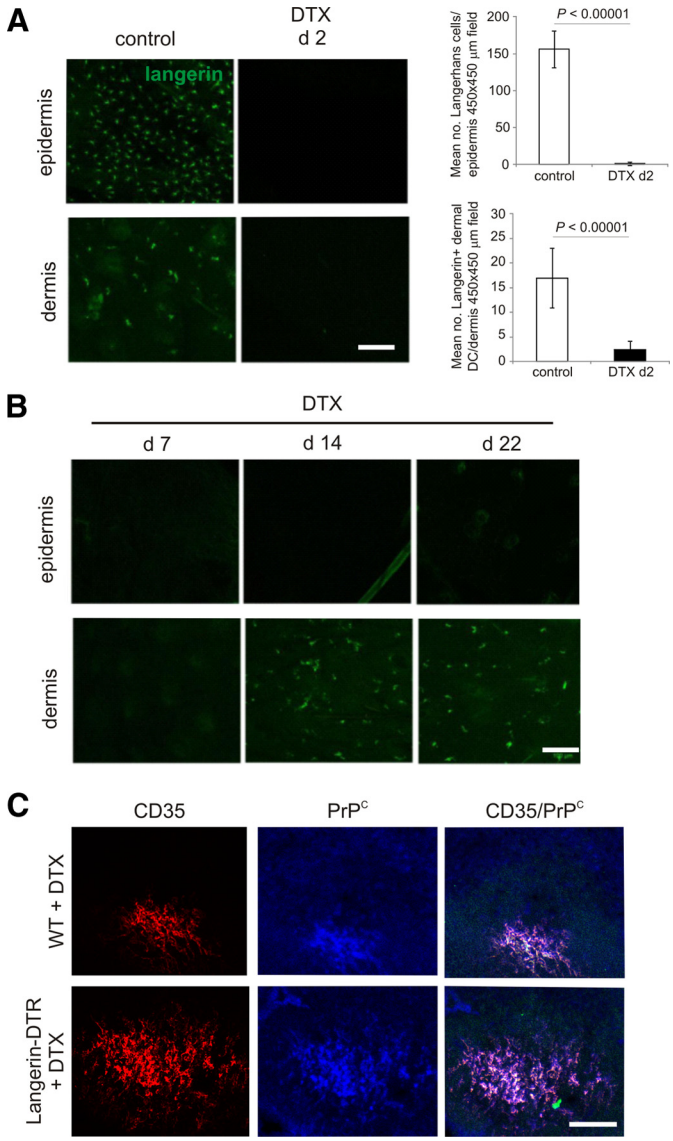

Figure 5. Effect of DTX treatment on the status of langerin$^+$ cells in the skin and FDCs in the LNs of langerin-DTR mice. (A) Epidermal LCs and langerin$^+$ dermal DCs are significantly depleted within 2 days (d 2) after DTX treatment of langerin-DTR mice. Histograms show the effects of DTX treatment on the mean number of LCs in the epidermis and langerin$^+$ DCs in the dermis (expressed as mean no. cells±SD/450×450 μm field of view). In each instance, three mice/group were analyzed and data collected from four images/mouse. (B) Epidermal LCs and langerin$^+$ dermal DCs remain depleted in langerin-DTR mice until at least 14 days after DTX treatment. (C) No observable effect of DTX treatment on the status of FDCs in LNs from langerin-DTR mice was observed. Data are representative of tissues from at least three mice/group. Original scale bars = 100 μm.

Determining the fate of PrP^{Sc} after infection by skin scarification

To track the cellular sites of PrP^{Sc} uptake within the skin after infection by skin scarification, highly PrP^{Sc}-enriched, scrapie-associated fibrils were isolated from the brains of mice with clinical prion disease and fluorescently tagged with Alexa-Fluor

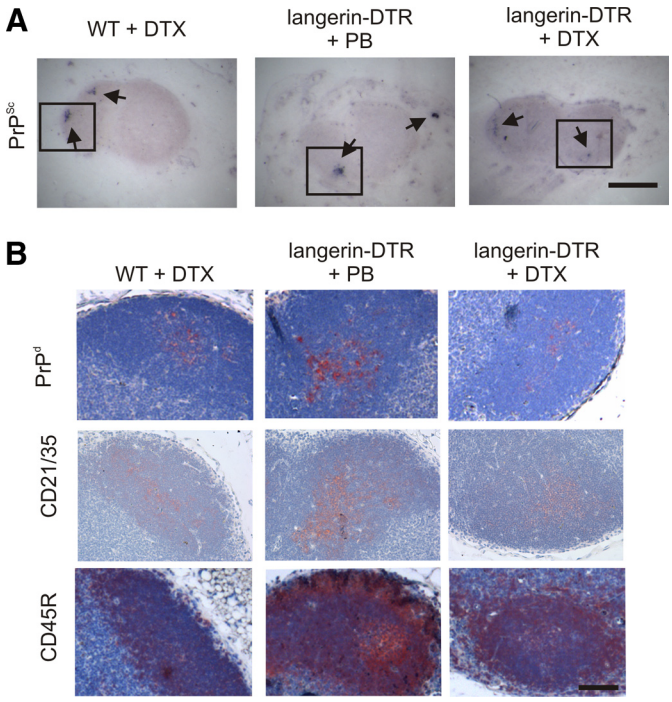

Figure 6. No effect of langerin$^+$ cell depletion on the early accumulation of prions in the draining LN. Langerin-DTR mice were injected with DTX to deplete their langerin$^+$ cells, and 2 days later, mice were exposed to ME7 scrapie prions by skin scarification. DTX-treated WT mice and PB-treated langerin-DTR mice were used as controls. Draining LNs were collected 35 days postinfection (n=3 mice/group). (A) No effect of langerin$^+$ cell depletion on the early accumulation of PrP^{Sc} (blue/black) upon FDC (arrows) within the draining LN was observed. (B) Boxed area in A is shown at greater magnification. Analysis of adjacent sections confirmed that the PrP^d (red, top panels) was in association with FDC (CD21/35-expressing cells; red, middle panels). Original scale bars = 500 μm (A); 100 μm (B).

546 dye (**Fig. 8A**), as described [26], to enable their visualization in tissues by immunofluorescent confocal microscopy (Fig. 8B). Following fluorescent-tagging, PK treatment, and gel electrophoresis, PrP^{Sc} samples were analyzed by silver-staining (Fig. 8A, left panel), fluorograph (Fig. 8A, middle panel), and PrP-specific immunoblot (Fig. 8A, right panel). Although comparison of the silver-stained gel with the immunoblot indicated that there were many other proteins besides PrP^{Sc} in the non-

TABLE 2. Effect of langerin$^+$ Cell Depletion on Prion Disease Susceptibility

Mouse strain	Treatment[a]	Incidence[b]	Mean incubation period (days) ± SE
WT	DTX	8/8	350 ± 12
Langerin-DTR	PBS	8/8	332 ± 6
Langerin-DTR	DTX	7/7	347 ± 7

[a] Mice were treated with DTX, 2 days before infection with ME7 scrapie prions via skin scarification. [b] Incidence, Number of animals affected with clinical prion disease/number of animals tested.

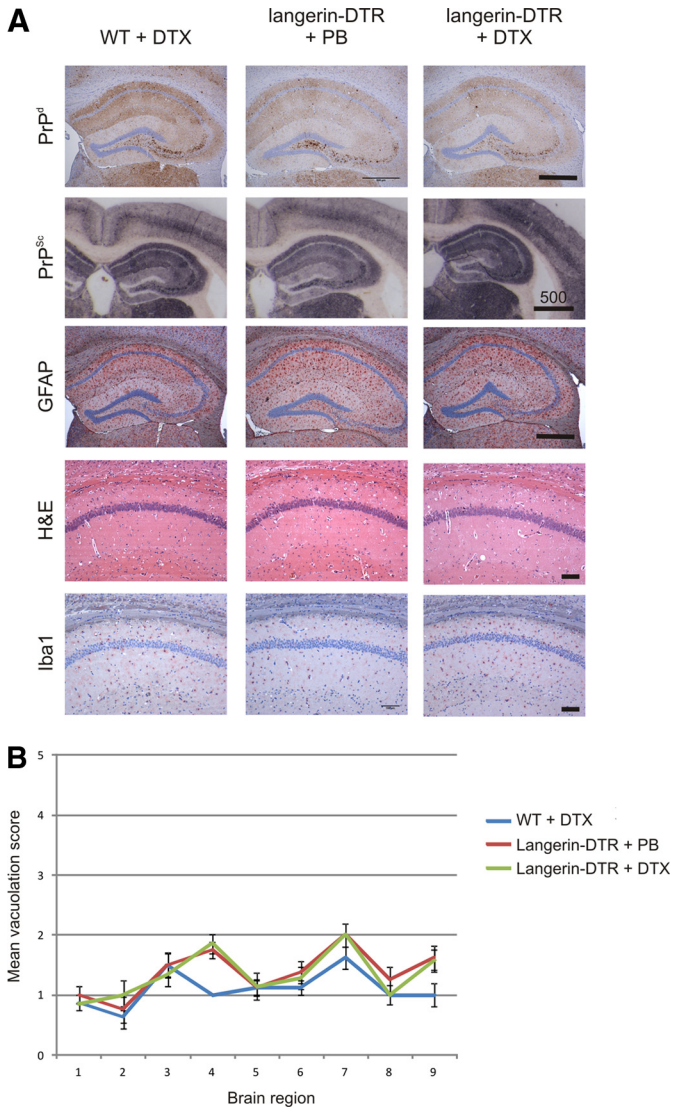

Figure 7. Effect of langerin$^+$ cell depletion on the development of neuropathology within the brain. Langerin-DTR mice were injected with DTX to deplete their langerin$^+$ cells, and 2 days later, mice were exposed to ME7 scrapie prions by skin scarification. DTX-treated WT mice and PB-treated langerin-DTR mice were used as controls. Brains were collected from clinically, scrapie-affected mice at the end of the experiment and the neuropathology within each brain compared. (A) Heavy accumulations of disease-specific PrP (brown, top row), reactive astrocytes expressing GFAP (red, third row from top), high levels of spongiform pathology (H&E, fourth row from top), and active microglia-expressing Iba-1 (red, bottom row) were detected in the brains of all clinically, scrapie-affected mice. Analysis of adjacent sections by PET immunoblot analysis confirmed the presence of PK-resistant PrP^{Sc} (blue/black, second row from top). Original scale bars = 100 μm unless indicated. (B) Pathological assessment of the spongiform change (vacuolation) in brains from terminally scrapie-affected mice. Vacuolation was scored on a scale of 0–5 in the following gray matter areas: G1, dorsal medulla; G2, cerebellar cortex; G3, superior colliculus; G4, hypothalamus; G5, thalamus; G6, hippocampus; G7, septum; G8, retrosplenial and adjacent motor cortex; G9, cingulate and adjacent motor cortex. Data are representative of tissues from seven to eight mice/group.

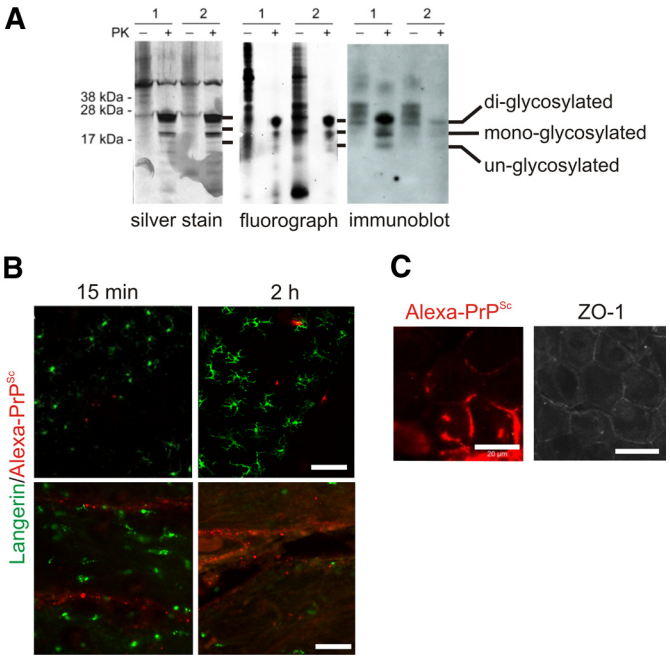

Figure 8. Histolopathological analysis of the distribution of PrP^{Sc} within the skin after exposure via scarification. (A) Highly PrP^{Sc}-enriched, scrapie-associated fibrils were isolated from the brains of mice with clinical prion disease and fluorescently tagged with Alexa-Fluor 546 dye as described [26]. Following PK treatment and gel electrophoresis, samples were analyzed by silver-staining (left panel), fluorograph (panel), and PrP-specific immunoblot (right panel). Fluorograph analysis confirmed that in the PK-treated samples, the Alexa-Fluor 546 dye was bound only to PrP^{Sc}. After PK treatment of PrP^{Sc}, a typical three-band pattern was observed between molecular mass values of 20 and 30 kDa on the PrP-specific immunoblot and the fluorograph, representing unglycosylated, monoglycosylated, and diglycosylated isomers of PrP (in order of increasing molecular mass). Figures above gels represent individual preparations. (B) Mice were exposed to Alexa-PrP^{Sc} by skin scarification and ears collected at the times indicated and tissues analyzed by confocal microscopy. Whole-mount IHC analysis of epidermal and dermal ear skin sheets from the site of scarification suggested that there was no direct association of LCs in the epidermis (upper panels) or langerin$^+$ cells in the dermis (lower panels) with the Alexa-PrP^{Sc}. (C) IHC of whole-mount, immunostained sheets prepared from Alexa-PrP^{Sc}-exposed mice suggested that the PrP^{Sc} (red, left panel) was associated with the intercellular spaces between keratinocytes where the ZO-1-expressing tight junctions are located (white, right panel). Data are representative of tissues from four mice/group. (B) Original scale bars = 50 μm (upper panels) and 100 μ m (lower panels); (C) 20 μm.

PK-treated (−) samples, fluorograph analysis confirmed that in the PK-treated (+) samples, the Alexa-Fluor 546 dye was bound only to PrP^{Sc}. The PK-treated Alexa-Fluor 546 dye-labeled PrP^{Sc} preparations are referred to as Alexa-PrP^{Sc} hereafter and used in the experiments below.

Immunofluorescent confocal analysis showed that Alexa-PrP^{Sc} was readily detected within the skin at the site of scarification within 15 min of exposure and was observable for up to at least 24 h (Fig. 8B and Supplemental Fig. 1B). We therefore determined whether the Alexa-PrP^{Sc} was acquired by LCs in the epidermis or langerin$^+$ cells in the dermis. IHC analysis suggested that there was no direct association of LCs with the Alexa-PrP^{Sc} (Fig. 8B). Similarly, no association of Alexa-PrP^{Sc} with langerin$^+$ cells in the dermis was observed. Taken together, these data clearly show that langerin$^+$ cells do not acquire PrP^{Sc} after exposure. These data are congruent with data above showing that the specific depletion of langerin$^+$ cells does not influence prion neuroinvasion from the skin. As it would not be possible to definitively determine where any Alexa-PrP^{Sc}-bearing cells within the draining LN had acquired the PrP^{Sc}, FACS analysis of LNs from Alexa-PrP^{Sc}-exposed mice was not undertaken. Any Alexa-PrP^{Sc} associated with mononuclear phagocytes in the draining LN may have been acquired: by cells within the skin before their subsequent migration to the LN; after the cell-free dissemination of Alexa-PrP^{Sc} to the LN; or simply, acquired by bystander cells during preparation of cell suspensions for FACS analysis.

Cells within the epidermis are sealed by tight junctions that help to protect the skin from water and solute transfer, pathogens, and particulate antigens [38]. Closer scrutiny of epidermal sheets prepared from Alexa-PrP^{Sc}-exposed mice suggested that some of the PrP^{Sc} was associated with the intercellular spaces between keratinocytes, where the tight junction barrier (as revealed by ZO-1) was located (Fig. 8C).

Further histological analysis of scarified skin demonstrated a peracute-localized dermatitis at the site of scarification by 15 min after treatment, which was more pronounced by 2 h when the presence of an inflammatory exudate was noted (Supplemental Fig. 1A). Neutrophils were sparsely distributed within skin from control mice and were rare within the skin in regions distal from the site of exposure. However, a prominent infiltration of neutrophils into the site of scarification was observed at 2 h (Supplemental Fig. 1A). This observation was consistent with the up-regulation of many genes associated with neutrophil chemotaxis and function identified from the microarray analysis of skin collected 2 h after scarification when compared with intact (control) skin (Supplemental Tables 1 and 2). These data clearly show that scarification leads to the up-regulation of genes encoding neutrophil chemoattractants, which stimulate the rapid migration of neutrophillic granulocytes to the lesion site. Indeed, a significant influx of neutrophils was observed within the site of exposure in close association with the Alexa-PrP^{Sc} (Supplemental Fig. 1B).

DISCUSSION

How prions are propagated from the skin to the draining LN after exposure via skin scarification is uncertain. Data in this study clearly demonstrate that langerin$^+$ cells, including LCs and langerin$^+$ classical DCs, do not play a role, as their specific depletion did not influence prion pathogenesis. These data are congruent with data from our previous study, which suggested that prion neuroinvasion from the skin was not influenced when LC migration from the skin was impeded [23]. However, our data show that the depletion of a nonepidermal CD11c$^+$ cell population impaired the early accumulation of prions in the draining LN. Histological and microarray analysis of the skin demonstrated that scarification resulted in the up-regulation of many genes associated with the activity of neutro-

phillic granulocytes. As a consequence, neutrophils were abundant within the scarification site and in close association with PrP^{Sc}. Whether neutrophils may likewise influence prion neuroinvasion from the skin is uncertain and remains to be determined. However, the possibility that prions may also be delivered to the draining LN independently of $CD11c^+$ cells or cell-free—for example, as a complement-opsonized complex—cannot be excluded. Together, these data suggest that the propagation of prions from the skin to the draining LN occurs via dermal classical DCs, independently of $langerin^+$ cells. However, the influence of other $langerin^+$ cell-independent mechanisms cannot be excluded entirely. Identification of the precise cellular and molecular mechanisms by which prions are propagated from the site of exposure to the draining lymphoid tissues in which they replicate before neuroinvasion may identify novel factors that influence disease susceptibility or targets for intervention in peripherally acquired infections.

The identity of the $CD11c^+$ $langerin^-$ cell population that influences the propagation of prions from the skin is uncertain, and further studies are necessary to address this issue. Unfortunately, it was only practically possible to use the CD11c-DTR mice as bone marrow donors to create CD11c-DTR → WT mice, as CD11c-DTR mice (alone) develop a spontaneous lethality, ~7 days after DTX treatment. This affect is not observed in Langerin-DTR mice, even after multiple doses of DTX [21]. As a consequence, we were unable to study prion pathogenesis in the temporary absence of all $CD11c^+$ cell lineages at the time of exposure. The dermal classical DCs have been shown to be highly mobile and to continuously survey the dermis to detect pathogens [39]. Thus, it is plausible that $CD11c^+$ $langerin^-$ DCs migrating through the dermis may likewise acquire prions and deliver them to FDCs within the draining LN. Alternatively, it has been reported that classical DCs may also promote prion transfer directly to neurons [40]. Interactions between classical DCs and the peripheral nervous system have been described [41, 42]. Studies have also shown that bone marrow-derived DCs can form tunneling, nanotube-like structures when cocultured with primary neurons facilitating the intracellular transfer of prions between these cells [26, 43]. However, whether classical DCs do play an important role in the transfer of prions from the immune to the peripheral nervous system in vivo is uncertain, as subsequent data suggested classical DCs, B cells, or other mononuclear cells were unlikely to have a major influence [44].

Chemokines and chemokine receptors play important roles in attracting classical DCs to the draining LNs and controlling their positioning within them. The chemokines CCL19 and CCL21 are constitutively expressed within the LN T cell zones and mediate the homing of chemokine receptor CCR7-expressing, naïve T cells and classical DCs into these regions [45]. Data show that prion pathogenesis after s.c. exposure is not affected in *plt/plt* mice with impaired, CCL19/CCL21-mediated classical DC migration into T cell zones [46]. These data are consistent with other studies showing that prion disease pathogenesis is not influenced in mice deficient in T cells [36, 47–49]. In contrast, the chemokine CXCL13 is highly expressed by FDCs and adjacent follicular stromal cells in the B cell follicles and modulates the homing of CXCR5-expressing B cells into these regions [50]. Dermal DCs migrating from the skin also express high levels of CXCR5 and migrate into the FDC-containing B cell follicles in response to CXCL13 stimulation [51]. The precise fate of the prions, following their uptake and transport to the draining lymphoid tissue via DCs, is uncertain. Whether the production of CXCL13 by FDC stimulates the migration of prion-bearing, CXCR5-expressing classical DCs directly into the B cell follicles, leading to the subsequent infection of FDC, remains to be determined.

Certain tissue macrophage populations, such as those in the peritoneal cavity, the lamina propria of the intestine, the SCS, and the splenic marginal zone, also express low levels of CD11c. Accordingly, these macrophage populations are likewise depleted in CD11c-DTR mice [52, 53]. The SCS macrophages appear to be specialized to capture antigen-containing immune complexes arriving in the LN via cell processes that they extend into the lumen of the SCS [54–58]. The SCS macrophages are a distinct, poorly endocytic and degradative macrophage subset [58]. In contrast to other macrophage subsets, SCS macrophages retain immune complexes on their surfaces for rapid translocation through the SCS floor to underlying follicular B cells. These B cells then acquire the immune complexes via their CRs and deliver them to FDCs. The shuttling of immune complexes via the SCS macrophage–B cell cellular relay represents an efficient route through which antigens are delivered to FDCs. Prions are also considered to be acquired by FDCs as complement-bound complexes [34, 59–61]. These characteristics suggest that SCS macrophages in LNs (and their counterparts in the spleen) may also aid the delivery of complement-bound prions to FDCs. Indeed, disease-specific PrP has been detected in association with SCS macrophages in the mesenteric LNs of prion-exposed sheep [62]. The SCS macrophages and their counterparts in the splenic marginal zone express high levels of sialoadhesin (CD169). Although these cells are depleted efficiently and significantly in CD11c-DTR mice [52, 53], our IHC analysis shows that in contrast to classical DCs, $CD169^+$ cells were not depleted significantly in DTX-treated, CD11c-DTR → WT mice. These data suggest that the effects of DTX treatment on the early accumulation of prions within the draining LNs of CD11c-DTR → WT mice were not a result of the depletion of $CD169^+$ $CD11c^+$ $langerin^-$ SCS macrophages.

Although classical DCs were efficiently depleted in DTX-treated, CD11c-DTR → WT mice (Fig. 1B), the early accumulation of prions within the draining LN was partially impaired, and the mice succumbed to clinical prion disease. Further studies using larger groups of CD11c-DTR → WT mice will be required to determine whether the absence of a significant effect on the onset of clinical disease was a result of variance in the survival times of the DTX-treated mice. However, our data suggest that other $CD11c^+$ cell-independent mechanisms may also contribute to the propagation of prions from the skin to the draining LN. Neutrophil infiltration was a prominent feature after skin scarification. Large numbers of neutrophils were observed within the site of scarification, in close association with the Alexa-PrP^{Sc} (Supplemental Fig. 1), consistent with the demonstration of PrP^{Sc} in association with neutrophils in the afferent lymph of sheep after exposure via the

same route [63]. Of course, further studies, for example, using neutropenic mice, are required to determine whether neutrophils influence prion neuroinvasion from the skin. The impaired prion accumulation in the draining LNs of DTX-treated CD11c-DTR → WT is highly unlikely to be a result of depletion of neutrophils, as these cells do not express CD11c and are not depleted in DTX-treated CD11c-DTR mice [19, 64].

The possibility cannot be excluded that a significant fraction of the prions in the initial inoculum may also be delivered to the draining LN cell-free, for example, as a complement-opsonized complex. Analysis of the distribution of Alexa-PrP^{Sc} within the layers of the skin after exposure suggested accumulation between keratinocytes in regions associated with the tight junction paracellular diffusion barrier (Fig. 8C). Thus, it is plausible that disruptions to this barrier as a consequence of scarification may lead to the penetrance of prions into the underlying tissue and their dissemination via afferent lymph to the draining LN.

In conclusion, our data suggest that the propagation of prions from the skin to the draining LN occurs via dermal classical DCs, independently of langerin$^+$ cells. However, the influence of other langerin$^+$ cell-independent mechanisms cannot be excluded entirely. Indeed, the possibility that prions may also be delivered to the draining LN cell-free, for example, as a complement-opsonized complex within the afferent lymph, cannot be excluded. Identification of the precise cellular and molecular mechanisms by which prions are propagated from the site of exposure to the draining lymphoid tissues, in which they replicate before neuroinvasion, may pinpoint novel factors that influence disease susceptibility and targets for intervention in peripherally acquired infections.

AUTHORSHIP

N.A.M. conceived of the study. N.A.M. and G.J.W. designed the study, performed experiments, analyzed data, and contributed to writing. A.K., B.M., and C.Z. contributed to the design of the study, data analysis, and the writing.

ACKNOWLEDGMENTS

N.A.M. and work in this study were supported by project and Institute Strategic Programme grant funding from the Biotechnology and Biological Sciences Research Council. C.Z. and N.A.M. are also supported by funding from the European Union FP7 (PRIORITY; Grant Agreement 222,887). We thank Karen Brown, Bob Fleming, Andrew Gill, Pip Beard, Fraser Laing, Irene McConnell, Mary Brady, Simon Cumming, Darren Shaw, and the Pathology Services Group (University of Edinburgh, UK), Duncan Browman (Institut Pasteur, Paris, France), and Keisuke Nagao (Keio University School of Medicine, Tokyo, Japan) for excellent technical support; Steffen Jung (Weizmann Institute of Science, Rehovot, Israel) for provision of CD11c-DTR transgenic mice; Mikio Furuse (Kobe University Graduate School of Medicine, Japan) for provision of anti-ZO-1 mAb; and John Hopkins (University of Edinburgh, UK) for helpful discussion.

DISCLOSURES

The authors declare no competing financial conflict of interest.

REFERENCES

1. Mabbott, N. A., Mackay, F., Minns, F., Bruce, M. E. (2000) Temporary inactivation of follicular dendritic cells delays neuroinvasion of scrapie. *Nat. Med.* **6,** 719–720.
2. Montrasio, F., Frigg, R., Glatzel, M., Klein, M. A., Mackay, F., Aguzzi, A., Weissmann, C. (2000) Impaired prion replication in spleens of mice lacking functional follicular dendritic cells. *Science* **288,** 1257–1259.
3. Mohan, J., Bruce, M. E., Mabbott, N. A. (2005) Follicular dendritic cell dedifferentiation reduces scrapie susceptibility following inoculation via the skin. *Immunology* **114,** 225–234.
4. Glaysher, B. R., Mabbott, N. A. (2007) Role of the draining lymph node in scrapie agent transmission from the skin. *Immunol. Lett.* **109,** 64–71.
5. Andreoletti, O., Berthon, P., Marc, D., Sarradin, P., Grosclaude, J., van Keulen, L., Schelcher, F., Elsen, J-M., Lantier, F. (2000) Early accumulation of PrP^{Sc} in gut-associated lymphoid and nervous tissues of susceptible sheep from a Romanov flock with natural scrapie. *J. Gen. Virol.* **81,** 3115–3126.
6. Sigurdson, C. J., Williams, E. S., Miller, M. W., Spraker, T. R., O'Rourke, K. I., Hoover, E. A. (1999) Oral transmission and early lymphoid tropism of chronic wasting disease PrP^{res} in mule deer fawns (*Odocoileus hemionus*). *J. Gen. Virol.* **80,** 2757–2764.
7. Mabbott, N. A., Young, J., McConnell, I., Bruce, M. E. (2003) Follicular dendritic cell dedifferentiation by treatment with an inhibitor of the lymphotoxin pathway dramatically reduces scrapie susceptibility. *J. Virol.* **77,** 6845–6854.
8. Prinz, M., Huber, G., Macpherson, A. J. S., Heppner, F. L., Glatzel, M., Eugster, H-P., Wagner, N., Aguzzi, A. (2003) Oral prion infection requires normal numbers of Peyer's patches but not of enteric lymphocytes. *Am. J. Pathol.* **162,** 1103–1111.
9. Glaysher, B. R., Mabbott, N. A. (2007) Role of the GALT in scrapie agent neuroinvasion from the intestine. *J. Immunol.* **178,** 3757–3766.
10. McCulloch, L., Brown, K. L., Bradford, B. M., Hopkins, J., Bailey, M., Rajewsky, K., Manson, J. C., Mabbott, N. A. (2011) Follicular dendritic cell-specific prion protein (PrP^C) expression alone is sufficient to sustain prion infection in the spleen. *PLoS Pathog.* **7,** e1002402.
11. Bolton, D. C., McKinley, M. P., Prusiner, S. B. (1982) Identification of a protein that purifies with the scrapie prion. *Science* **218,** 1309–1311.
12. Legname, G., Baskakov, I. V., Nguyen, H-O. B., Riesner, D., Cohen, F. E., DeArmond, S. J., Prusiner, S. B. (2004) Synthetic mammalian prions. *Science* **305,** 673–676.
13. Hunter, N., Foster, J., Chong, A., McCutcheon, S., Parnham, D., Eaton, S., MacKenzie, C., Houston, F. (2002) Transmission of prion diseases by blood transfusion. *J. Gen. Virol.* **83,** 2897–2905.
14. Glatzel, M., Heppner, F. L., Albers, K. M., Aguzzi, A. (2001) Sympathetic innervation of lymphoreticular organs is rate limiting for prion neuroinvasion. *Neuron* **31,** 25–34.
15. Steinman, R. M., Nussenzweig, M. C. (2002) Avoiding horror autotoxicus: the importance of dendritic cells in peripheral T cell tolerance. *Proc. Natl. Acad. Sci. USA* **99,** 351–358.
16. Henri, S., Poulin, L. F., Tamoutounour, S., Ardouin, L., Guillams, M., de Bovis, B., Devilard, E., Viret, C., Azukizawa, H., Kissenpfennig, A., Malissen, B. (2009) CD207+ CD103+ dermal dendritic cells cross-present keratinocyte-derived antigens irrespective of the presence of Langerhans cells. *J. Exp. Med.* **207,** 189–206.
17. Ho, L-J., Wang, J-J., Shaio, M-F., Kao, C-L., Chang, D-M., Han, S-W., Lai, J-H. (2001) Infection of human dendritic cells by dengue virus causes cell maturation and cytokine production. *J. Immunol.* **166,** 1499–1506.
18. Ho, A. W., Prabhu, N., Betts, R. J., Ge, M. Q., Dai, X., Hutchinson, P. E., Lew, F. C., Wong, K. L., Hanson, B. J., Macary, P. A., Kemeny, D. M. (2011) Lung CD103+ dendritic cells efficiently transport influenza virus to the lymph node and load viral antigen onto MHC class I for presentation to CD8 T cells. *J. Immunol.* **187,** 6011–6021.
19. Raymond, C. R., Aucouturier, P., Mabbott, N. A. (2007) In vivo depletion of CD11c$^+$ cells impairs scrapie agent neuroinvasion from the intestine. *J. Immunol.* **179,** 7758–7766.
20. Cordier-Dirikoc, S., Chabry, J. (2008) Temporary depletion of CD11c+ dendritic cells delays lymphoinvasion after intraperitoneal scrapie infection. *J. Virol.* **82,** 8933–8936.
21. Kissenpfennig, A., Henri, S., Dubois, B., Laplace-Builhè, C., Perrin, P., Romani, N., Tripp, C. H., Douillard, P., Leserman, L., Kaiserlian, D., Saeland, S., Davoust, J., Malissen, B. (2005) Dynamics and function of Langerhans cells in vivo: dermal dendritic cells colonize lymph node areas distinct from slower migrating Langerhans cells. *Immunity* **22,** 643–654.
22. Jung, S., Unutmaz, D., Wong, P., Sano, G-I., De los Santos, K., Sparwasser, T., Wu, S., Vuthoori, S., Ko, K., Zavala, F., Pamer, E. G., Littman, D. R., Lang, R. A. (2002) In vivo depletion of CD11c$^+$ dendritic cells abrogates priming of CD8$^+$ T cells by exogenous cell-associated antigens. *Immunity* **17,** 211–220.

23. Mohan, J., Bruce, M. E., Mabbott, N. A. (2005) Neuroinvasion by scrapie following inoculation via the skin is independent of migratory Langerhans cells. *J. Virol.* **79,** 1888–1897.
24. Fraser, H., Dickinson, A. G. (1973) Agent-strain differences in the distribution and intensity of grey matter vacuolation. *J. Comp. Pathol.* **83,** 29–40.
25. Fraser, H., Dickinson, A. G. (1968) The sequential development of the brain lesions of scrapie in three strains of mice. *J. Comp. Pathol.* **78,** 301–311.
26. Gousset, K., Schiff, E., Langevin, C., Marijanovic, Z., Caputo, A., Browman, D. T., Chanouard, N., de Chaumont, F., Martino, A., Enninga, J., Olivio-Marin, J-C., Männel, D., Zurzolo, C. (2009) Prions hijack tunnelling nanotubes for intercellular spread. *Nat. Cell Biol.* **11,** 328–336.
27. Zanusso, G., Liu, D., Ferrari, S., Hegyi, I., Yin, X., Aguzzi, A., Hornemann, S., Liemann, S., Glockshuber, R., Manson, J. C., Brown, P., Petersen, R. B., Gambetti, P., Sy, M-S. (1998) Prion protein expression in different species: analysis with a panel of new mAbs. *Proc. Natl. Acad. Sci. USA* **95,** 8812–8816.
28. Nagao, K., Ginhoux, F., Leitner, W. W., Motegi, S-I., Bennet, C. L., Clausen, B. J., Merad, M., Udey, M. C. (2009) Murine epidermal Langerhans cells and langerin-expressing dermal dendritic cells are unrelated and exhibit distinct functions. *Proc. Natl. Acad. Sci. USA* **106,** 3312–3317.
29. Itoh, M., Yonemura, S., Nagafuchi, A., Tsukita, S., Tsukita, S. (1991) A 220-kD undercoat-constitutive protein: its specific localization at cadherin-based cell-cell adhesion sites. *J. Cell Biol.* **115,** 1449–1462.
30. Farquhar, C. F., Somerville, R. A., Ritchie, L. A. (1989) Post-mortem immunodiagnosis of scrapie and bovine spongiform encephalopathy. *J. Virol. Met.* **24,** 215–222.
31. McBride, P., Eikelenboom, P., Kraal, G., Fraser, H., Bruce, M. E. (1992) PrP protein is associated with follicular dendritic cells of spleens and lymph nodes in uninfected and scrapie-infected mice. *J. Pathol.* **168,** 413–418.
32. Schulz-Schaeffer, W. J., Tschoke, S., Kranefuss, N., Drose, W., Hause-Reitner, D., Giese, A., Groschup, M. H., Kretzschmar, H. A. (2000) The paraffin-embedded tissue blot detects PrP^{sc} early in the incubation time in prion diseases. *Am. J. Pathol.* **156,** 51–56.
33. Ginhoux, F., Collin, M. P., Bogunovic, M., Abel, M., Leboeuf, M., Helft, J., Ochando, J., Kissenpfennig, A., Malissen, B., Grisotto, M., Snoeck, H., Randolph, G., Merad, M. (2007) Blood-derived dermal langerin+ dendritic cells survey the skin in the steady state. *J. Exp. Med.* **204,** 3133–3146.
34. Zabel, M. D., Heikenwalder, M., Prinz, M., Arrighi, I., Schwarz, P., Kranich, J., von Teichman, A., Haas, K. M., Zeller, N., Tedder, T. F., Weiss, J. H., Aguzzi, A. (2007) Stromal complement receptor CD21/35 facilitates lymphoid prion colonization and pathogenesis. *J. Immunol.* **179,** 6144–6152.
35. Brown, K. L., Stewart, K., Ritchie, D., Mabbott, N. A., Williams, A., Fraser, H., Morrison, W. I., Bruce, M. E. (1999) Scrapie replication in lymphoid tissues depends on PrP-expressing follicular dendritic cells. *Nat. Med.* **5,** 1308–1312.
36. Klein, M. A., Frigg, R., Raeber, A. J., Flechsig, E., Hegyi, I., Zinkernagel, R. M., Weissmann, C., Aguzzi, A. (1998) PrP expression in B lymphocytes is not required for prion neuroinvasion. *Nat. Med.* **4,** 1429–1433.
37. Mabbott, N. A., Bailie, J. K., Kobayashi, A., Donaldson, D. S., Ohmori, H., Yoon, S.-O., Freedman, A. S., Freeman, T. C., Summers, K. M. (2011) Expression of mesenchyme-specific gene signatures by follicular dendritic cells: insights from the meta-analysis of microarray data from multiple mouse cell populations. *Immunology* **133,** 482–498.
38. Kubo, A., Nagao, K., Yokouchi, M., Sasaki, H., Amagai, Y. (2009) External antigen uptake by Langerhans cells with reorganization of epidermal tight junction barriers. *J. Exp. Med.* **206,** 2937–2946.
39. Ng, L. G., Hsu, A., Mandell, M. A., Roediger, B., Hoeller, C., Mrass, P., Iparraguirre, A., Cavanagh, L. L., Triccas, J. A., Beverley, S. M., Scott, P., Weninger, W. (2008) Migratory dermal dendritic cells act as rapid sensors of protozoan parasites. *PLoS Pathog.* **4,** e1000222.
40. Aucouturier, P., Geissmann, F., Damotte, D., Saborio, G. P., Meeker, H. C., Kascsak, R., Kascsak, R., Carp, R. I., Wisniewski, T. (2001) Infected splenic dendritic cells are sufficient for prion transmission to the CNS in mouse scrapie. *J. Clin. Invest.* **108,** 703–708.
41. Defaweux, V., Dorban, G., Demonceau, C., Piret, J., Jolois, O., Thellin, O., Thielen, C., Heinen, E., Antoine, N. (2005) Interfaces between dendritic cells, other immune cells, and nerve fibres in mouse Peyer's patches: potential sites for neuroinvasion in prion diseases. *Micro. Res. Tech.* **66,** 1–9.
42. Dorban, G., Defaweux, V., Levavasseur, E., Demonceau, C., Thellin, O., Flandroy, S., Piret, J., Falisse, N., Heinen, E., Antoine, N. (2007) Oral scrapie infection modifies the homeostasis of Peyer's patches' dendritic cells. *Histochem. Cell Biol.* **128,** 243–251.
43. Langevin, C., Gousset, K., Costanzo, M., Richard-Le Goff, O., Zurzolo, C. (2010) Characterization of the role of dendritic cells in prion transfer to primary neurons. *Biochem. J.* **431,** 189–198.
44. Raymond, C. R., Mabbott, N. A. (2007) Assessing the involvement of migratory dendritic cells in the transfer of the scrapie agent from the immune to peripheral nervous systems. *J. Neuroimmunol.* **187,** 114–125.
45. Saeki, H., Moore, A. M., Brown, M. J., Hwang, S. T. (1999) Cutting edge: secondary lymphoid-tissue chemokine (SLC) and CC chemokine receptor 7 (CCR7) participate in the emigration pathway of mature dendritic cells from the skin to regional lymph nodes. *J. Immunol.* **162,** 2472–2475.
46. Levavasseur, E., Matharom, P., Dorban, G., Nakano, H., Kakiuchi, T., Carnaud, C., Sarradin, P., Aucouturier, P. (2007) Experimental scrapie in "plt" mice: an assessment of the role of dendritic-cell migration in the pathogenesis of prion diseases. *J. Gen. Virol.* **88,** 2353–2360.
47. McFarlin, D. E., Raff, M. C., Simpson, E., Nehlsen, S. H. (1971) Scrapie in immunologically deficient mice. *Nature* **233,** 336.
48. Fraser, H., Dickinson, A. G. (1978) Studies on the lymphoreticular system in the pathogenesis of scrapie: the role of spleen and thymus. *J. Comp. Pathol.* **88,** 563–573.
49. Klein, M. A., Frigg, R., Flechsig, E., Raeber, A. J., Kalinke, U., Bluethman, H., Bootz, F., Suter, M., Zinkernagel, R. M., Aguzzi, A. (1997) A crucial role for B cells in neuroinvasive scrapie. *Nature* **390,** 687–691.
50. Ansel, K. M., Ngo, V. N., Hyman, P. L., Luther, S. A., Forster, R., Sedgwick, J. D., Browning, J. L., Lipp, M., Cyster, J. (2000) A chemokine-driven feedback loop organizes lymphoid follicles. *Nature* **406,** 309–314.
51. Saeki, H., Wu, M., Olasz, E., Hwang, S. T. (2000) A migratory population of skin-derived dendritic cells expresses CXCR5, responds to B lymphocyte chemoattractant in vitro, and co-localizes to B cell zones in lymph nodes in vivo. *Eur. J. Immunol.* **30,** 2808–2814.
52. Probst, H. C., Tschannen, K., Odermatt, B., Schwendener, R., Zinkernagel, R. M., van den Broek, M. (2005) Histological analysis of CD11c-DTR/GFP mice after in vivo depletion of dendritic cells. *Clin. Exp. Immunol.* **141,** 398–404.
53. Bradford, B. M., Sester, D., Hume, D. A., Mabbott, N. A. (2011) Defining the anatomical localisation of subsets of the murine mononuclear phagocyte system using integrin alpha X (ITGAX) and colony stimulating factor 1 receptor (CSF1-R) expression fails to discriminate dendritic cells from macrophages. *Immunobiology* **216,** 1228–1237.
54. Phan, T. G., Grigorova, I., Okada, T., Cyster, J. G. (2007) Subcapsular encounter and complement-dependent transport of immune complexes by lymph node B cells. *Nat. Immunol.* **8,** 992–1000.
55. Carrasco, Y. R., Batista, F. D. (2007) B cells acquire particulate antigen in a macrophage-rich area at the boundary between the follicle and the subcapsular sinus of the lymph node. *Immunity* **27,** 1–12.
56. Junt, T., Moseman, E. A., Iannacone, M., Massberg, S., Lang, P. A., Boes, M., Fink, K., Henrickson, S. E., Shayakhmetov, D. M., Di Paolo, N. C., Van Rooijen, N., Mempel, T. R., Whelan, S. P., von Andrian, U. H. (2007) Subcapsular sinus macrophages in lymph nodes clear lymph-borne viruses and present them to antiviral B cells. *Nature* **450,** 110–116.
57. Roozendaal, R., Mempel, T. R., Pitcher, L. A., González, S. F., Verschoor, A., Mebius, R. E., Von Andrian, U. H., Carroll, M. C. (2009) Conduits mediate transport of low-molecular-weight antigen to lymph node follicles. *Immunity* **30,** 264–276.
58. Phan, T. G., Green, J. A., Gray, E. E., Xu, Y., Cyster, J. G. (2009) Immune complex relay by subcapsular sinus macrophages and noncognate B cells drives antibody affinity maturation. *Nat. Immunol.* **10,** 786–793.
59. Klein, M. A., Kaeser, P. S., Schwarz, P., Weyd, H., Xenarios, I., Zinkernagel, R. M., Carroll, M. C., Verbeek, J. S., Botto, M., Walport, M. J., Molina, H., Kalinke, U., Acha-Orbea, H., Aguzzi, A. (2001) Complement facilitates early prion pathogenesis. *Nat. Med.* **7,** 488–492.
60. Mabbott, N. A., Bruce, M. E., Botto, M., Walport, M. J., Pepys, M. B. (2001) Temporary depletion of complement component C3 or genetic deficiency of C1q significantly delays onset of scrapie. *Nat. Med.* **7,** 485–487.
61. Mabbott, N. A., Bruce, M. E. (2004) Complement component C5 is not involved in scrapie pathogenesis. *Immunobiology* **209,** 545–549.
62. Jeffrey, M., González, L., Espenes, A., Press, C. M., Martin, S., Chaplin, M., Davis, L., Landsverk, T., MacAldowie, C., Eaton, S., McGovern, G. (2006) Transportation of prion protein across the intestinal mucosa of scrapie-susceptible and scrapie-resistant sheep. *J. Pathol.* **209,** 4–14.
63. Gossner, A., Hunter, N., Hopkins, J. (2005) Role of lymph-borne cells in the early stages of scrapie agent dissemination from the skin. *Vet. Immunol. Immunopathol.* **109,** 267–278.
64. Tittel, A. P., Heuser, C., Ohliger, C., Knolle, P. A., Engel, D. R., Kurts, C. (2011) Kidney dendritic cells induce innate immunity against bacterial pyelonephritis. *J. Am. Soc. Nephrol.* **22,** 2139–2141.

KEY WORDS:
transmissible spongiform encephalopathy · Langerhans cells · dendritic cells · neutrophils · follicular dendritic cell · PrP